Generation of positively-momentum-correlated biphotons from spontaneous parametric down-conversion

Sujun Yun,[1] P. Xu,[1,*] J. S. Zhao,[1] Y. X. Gong,[2] Y. F. Bai,[1] J. Shi,[1] and S. N. Zhu[1]

[1]*National Laboratory of Solid State Microstructures and School of Physics, Nanjing University, Nanjing 210093, China*

[2]*Department of Physics, Southeast University, Nanjing 211189, China*

(Received 22 April 2012; published 29 August 2012)

We propose to generate a counter-Einstein-Podolsky-Rosen (CEPR) state which possesses a positively-correlated momentum and anticorrelated position directly from spontaneous parametric down-conversion. The general CEPR state is given under a tightly focused Gaussian pump based on type II noncritical phase matching. We analytically and numerically study how a positively-correlated momentum and anticorrelated position of a biphoton can be achieved by choosing the proper focal parameter of the pump. To verify the degree of entanglement of the CEPR state, we calculate its entanglement entropy and it shows a unique dependence on the pump's focal parameter. Suggestions for practical engineering of the state are also given. Furthermore, based on an ideal CEPR state, we deduce a type of erect quantum ghost imaging which can be applied as the entanglement criterion. This work gives applicable references to the spatial control of an entangled photon source in experiments and may stimulate the development of new types of quantum technologies.

DOI: 10.1103/PhysRevA.86.023852 PACS number(s): 42.65.Lm, 03.65.Ud, 42.50.Dv, 42.30.Va

I. INTRODUCTION

The famous "Einstein-Podolsky-Rosen (EPR) paradox" [1], based on simultaneous entanglement over a continuum of correlated position and anticorrelated momentum [2,3], has boosted the research from fundamental physics [4] to prosperous quantum technologies such as quantum imaging [5–7], quantum lithography [8–10], quantum metrology [11,12], and quantum computation [13]. A widely used method for generating the EPR state is by spontaneous parametric down-conversion (SPDC) from nonlinear crystals where the transverse correlation of momenta between the signal and the idler holds a strong anticorrelation when the pump is assumed to be plane wave,

$$|\Psi\rangle_{\mathrm{EPR}} = \int |\vec{q},-\vec{q}\rangle\, d\vec{q} = \int |\vec{\rho},\vec{\rho}\,\rangle\, d\vec{\rho}, \tag{1}$$

in which $\vec{\rho}$ and $\vec{q}$ represent the transverse position and transverse momentum of photons, respectively. However, according to the basic principle of quantum mechanics, there must exist a counterpart of the EPR state which exhibits a positively-correlated (or correlated for short) momentum and anticorrelated position. The maximally entangled one is described as

$$|\Psi\rangle_{\mathrm{CEPR}} = \int |\vec{q},\vec{q}\rangle\, d\vec{q} = \int |\vec{\rho},-\vec{\rho}\,\rangle\, d\vec{\rho}. \tag{2}$$

Since the correlations of momentum and position in Eq. (2) are just reverse to those of the original EPR state, the above two-photon state can be referred as the counter-EPR (CEPR) state.

There has been plenty of research focusing on manipulation of the position and momentum correlation of entangled photon pairs by proper preparation of the pump beam [14–19] or utilization of external optical elements [20–24]. Most works focus on the generation of an anticorrelated-momentum EPR state or how to minimize the momentum correlation. Very recently an interesting work brought people's attention to the CEPR state in which a positive momentum correlation is realized by Hong-Ou-Mandel interference after the generation of EPR photon pairs [25]. Here we propose to engineer the CEPR state directly from nonlinear crystals by utilizing a tightly focused pump beam. Based on type II noncritical phase matching, we analytically and numerically study how a correlated momentum and anticorrelated position can be achieved by choosing the proper focal parameter of the pump. Furthermore, by employing the entanglement entropy, the degree of entanglement of the CEPR state is studied and it shows a unique dependence on the focal parameter. Suggestions for practical engineering of a CEPR state with a high degree of entanglement are also given. Quantum ghost imaging utilizing the ideal CEPR state is calculated, which suggests that the erect ghost image can serve as the criterion for the CEPR state. Other potential applications of such a CEPR state are still under investigation.

Our paper is organized as follows. In Sec. II, the general two-photon state with a positively correlated momentum is given under the condition of a paraxial Gaussian pump. In Sec. III, the position correlations of this state are studied both analytically and numerically. There exists a good correspondence between momentum and position correlations. In Sec. IV, in order to denote the degree of entanglement of the CEPR state, the entanglement entropy of the two-photon state is calculated using the Schmidt decomposition method. This section also includes suggestions on how to engineer a CEPR state with a high degree of entanglement. In Sec.V, possible applications of the CEPR state are discussed. Quantum imaging based on an ideal CEPR state is calculated. Conclusions are drawn in Sec. VI.

II. THE GENERAL TWO-PHOTON STATE WITH A CORRELATED MOMENTUM

We give a general two-photon state with a correlated momentum under the condition of a paraxial Gaussian pump.

*pingxu520@nju.edu.cn

As we mainly study the property of the spatial correlation between the signal and the idler, it is convenient to work in a monochromatic approximation of them, which is further justified experimentally through the use of narrow-band interference filters. In the interaction picture, the Hamiltonian H_I is

$$H_I = \varepsilon_0 \int d^3r \chi^{(2)} E_p^{(+)} E_s^{(-)} E_i^{(-)} + \text{H.c.}, \tag{3}$$

where $\chi^{(2)}$ is the effective second-order nonlinear coefficient. $E^{(+)}$ and $E^{(-)}$ denote the positive- and negative-frequency parts of the electric-field operators, respectively. H.c. means the Hermitian conjugate. The pump is taken as Gaussian TEM_{00} and considered as a classical electric field for simplicity. It is focused and the beam waist w_0 is located at the center of the crystal. When propagating along the z axis in an optically uniform medium, the pump has a transverse intensity distribution that is everywhere a Gaussian. It can be represented in the scalar approximation as Ref. [26]

$$A(\vec{\rho},z) = \frac{Aw_0}{w(z)} e^{-\rho^2/w^2(z)} e^{ik\rho^2/2R(z)} e^{i\phi(z)}, \tag{4}$$

where $w(z) = w_0(1 + z^2/z_0^2)^{1/2}$ represents the $1/e$ radius of the field distribution. $2z_0 = w_0^2 k_p$ is the confocal length of the pump and k_p is the pump wave vector. $R(z) = z(1 + z_0^2/z^2)$ denotes the radius of curvature of the pump wave front. And $\phi(z) = -\arctan(z/z_0)$ represents the spatial variation of the pump's phase. The pump can be expressed by Fourier expansion in the transverse momentum q_p space:

$$E_p(\vec{\rho},z,t) = Ae^{i(k_p z - \omega_p t)} \int d^2q_p e^{-q_p^2(\frac{w_0^2}{4} + i\frac{z}{2k_p})} e^{i\vec{q}_p\cdot\vec{\rho}}. \tag{5}$$

According to Eq. (5), there are two limiting cases corresponding to the weakly and strongly focused pump. Here, we define a focal parameter $\xi = L/2z_0$, in which L is the length of the crystal along the pump propagating direction. One case is that when $\xi \ll 1$, i.e., $L \ll k_p w_0^2$, the pump is considered to be collimated, then Eq. (5) turns into $E(\vec{\rho},z,t) = Ae^{i(k_p z - \omega_p t)} \int d^2q_p e^{-\frac{q_p^2 w_0^2}{4}} e^{i\vec{q}_p\cdot\vec{\rho}}$, which implies the longitudinal momentum of pump $k_{pz} \approx k_p$. In this case, the amplitude of the pump electric field in Eq. (4) takes the form $Ae^{-\rho^2/w_0^2}$, which means that the curvature of the optical wave front, the accretion of the beam waist radius, and the angular divergence of the pump can be neglected. The opposite limiting case is that $\xi \gg 1$, i.e., $L \gg k_p w_0^2$, the term $e^{-i\frac{q_p^2}{2k_p}z}$ in Eq. (5) plays an important role, which means that, for a different transverse mode q_p, the propagation phase is different. In this case, the longitude momentum of pump $k_{pz} \approx k_p - q_p^2/2k_p$.

Whereas the produced signal and idler photons are treated quantum mechanically, their negative parts of the field operators are

$$E_j^{(-)}(\vec{\rho},z,t) = E_j \int d^2q_j e^{-i(k_{jz}z + \vec{q}_j\cdot\vec{\rho}_j)} e^{i\omega_j t} \hat{a}^\dagger(\vec{q}_j,\omega_j), \tag{6}$$

where $\hat{a}^\dagger(\vec{q}_j,\omega_j)$ $(j = s,i)$ is the creation operator with modes $(\vec{q}_j, \omega_j)$, and E_j is the normalization coefficient.

By inserting Eqs. (5) and (6) into Eq. (3), the wave function $|\Psi\rangle$ evaluated from first-order perturbation theory can be written as

$$|\Psi\rangle = \psi_0 \int d^2q_s \int d^2q_i E_p(\vec{q}_s + \vec{q}_i) H(\Delta k_z, L) \times \hat{a}^\dagger(\vec{q}_s,\omega_s)\hat{a}^\dagger(\vec{q}_i,\omega_i)|0\rangle. \tag{7}$$

In this equation all the slowly varying terms and constants are absorbed into ψ_0. The pump term $E_p(\vec{q}_s + \vec{q}_i) = e^{-|\vec{q}_s+\vec{q}_i|^2 w_0^2/4}$ implies that the conservation of transverse momenta is fulfilled in the SPDC process. And the phase-matching function $H(\Delta k_z, L)$ is

$$H(\Delta k_z, L) = \frac{\sin(\Delta k_z L/2)}{\Delta k_z/2} \equiv L\text{sinc}(\Delta k_z L/2), \tag{8}$$

in which $\Delta k_z = k_{pz} - k_{sz} - k_{iz}$. Under the assumption of a monochromatic signal and idler photons, the longitudinal components of wave vectors through Taylor expansions are $k_{z,o} = k_o - \frac{q_o^2}{2k_o}$ for ordinary light and $k_{z,e} = k_e(\omega,\theta) + \frac{\partial k_e(\omega,\theta)}{\partial \vec{q}_e}\cdot\vec{q}_e - \frac{q_e^2}{2k_e(\omega,\theta)}$ for extraordinary light at $\vec{q} = 0$ [27], where $\frac{\partial k_e(\omega,\theta)}{\partial \vec{q}_e} = \frac{\omega}{c}\frac{\partial n_e}{\partial \vec{q}_e} = \frac{\omega}{c}\frac{\partial \theta}{\partial \vec{q}_e}\frac{\partial n_e}{\partial \theta}$ (n_e is the refractive index of extraordinary light and θ is the angle between $\vec{k}_e$ and the optic axis). It is notable that the walk-off effect of extraordinary light generally brings the spatial distinguishability of photon pairs in type II phase matching under the focused pump [15]. However, in the current discussion, the walk-off term in $k_{z,e}$ can be neglected based on type II noncritical phase matching. This gives

$$\begin{aligned}\Delta k_z &= k_{p,z} - k_{s,z} - k_{i,z} \\ &= k_p - k_s - k_i - \frac{q_p^2}{2k_p} + \frac{q_s^2}{2k_s} + \frac{q_i^2}{2k_i}.\end{aligned} \tag{9}$$

Here we suppose that the transverse momentum is relatively small and meets the paraxial approximation. Also, the wave vectors of the pump, the signal, and the idler under the zero-order Taylor expansions are matched, namely, $k_p - k_s - k_i = 0$, the mismatching of wave vectors along the z axis is

$$\Delta k_z = \frac{1}{2\alpha k_p}|\vec{q}_s - \alpha\vec{q}_i|^2, \tag{10}$$

where $\alpha = k_s/k_i > 0$ determines the ratio between the signal's and the idler's transverse momenta.

Inserting Eq. (10) into Eq. (7) gives

$$|\Psi\rangle = \psi_0 L \int d^2q_s \int d^2q_i e^{-\frac{|\vec{q}_s+\vec{q}_i|^2}{4}w_0^2} \text{sinc}\frac{|\vec{q}_s - \alpha\vec{q}_i|^2 L}{4\alpha k_p} \times \hat{a}^\dagger(\vec{q}_s,\omega_s)\hat{a}^\dagger(\vec{q}_i,\omega_i)|0\rangle. \tag{11}$$

Similar expressions can also be found in Refs. [14,16–18], however, here the general two-photon state is deduced under a focused Gaussian pump. The pump function $E_p = e^{-\frac{|\vec{q}_s+\vec{q}_i|^2}{4}w_0^2}$ in Eq. (11) tends to exhibit an anticorrelation in transverse momentum, while the term of the phase-matching function $H = \text{sinc}\frac{|\vec{q}_s-\alpha\vec{q}_i|^2 L}{4\alpha k_p}$ tends to exhibit a positive one. Obviously the momentum or spatial correlation of the entangled two-photon state is mainly determined by the pump function and the phase-matching function. Under the condition of a thin crystal and collimated pump, the momentum bandwidth of the phase-matching function is much larger than that

of the pump, so the generated two-photon state is mainly determined by the pump beam and has an anticorrelation in momentum. Specifically when the pump momentum's full width $\frac{4}{w_0}$ (when E_p drops to its $1/e$) is much narrower than that of the phase-matching function $4\sqrt{\frac{\alpha\pi k_p}{L}}$ (which is defined as when the H function drops to its first zero point), that is, $2z_0 = w_0^2 k_p \gg \frac{L}{\alpha\pi}$ or $\xi = L/2z_0 \ll \alpha\pi$, the two-photon state shows a strong anticorrelation in momentum. In practical experiments, the standard EPR state is achieved under this condition [2,3]. For the case when the momentum bandwidth of the phase-matching function is close to that of the pump, it corresponds to a minimally entangled state and has been studied for optimal single-mode coupling [18]. Both of these cases have been well studied.

In this work we focus on the case where the bandwidth of the phase-matching function is much narrower than that of the pump. The momentum correlation will turn into a positive one. This requires a long crystal and a tightly focused pump. The relation $\lim_{L\to\infty} \sin(xL)/x = \pi\delta(x)$ allows us to re-express the phase-matching function $H(\Delta k_z, L)$ in Eq. (11) as

$$\lim_{L\to\infty} H(\Delta k_z, L) = \lim_{L\to\infty} \frac{\sin\left(\frac{|\vec{q}_s - \alpha\vec{q}_i|^2}{4\alpha k_p} L\right)}{\frac{|\vec{q}_s - \alpha\vec{q}_i|^2}{4\alpha k_p}} = 4\pi\alpha k_p \delta[(q_{sx} - \alpha q_{ix})^2 + (q_{sy} - \alpha q_{iy})^2]. \tag{12}$$

According to Eq. (12), the general entangled two-photon state as shown in Eq. (11) becomes

$$|\Psi\rangle \sim \int d^2q e^{-(1+\alpha)^2 w_0^2 q^2/4} \hat{a}^\dagger(\alpha\vec{q}, \omega_s)\hat{a}^\dagger(\vec{q}, \omega_i)|0\rangle. \tag{13}$$

From Eq. (13), we can see that the two-photon wave packet cannot be factorized. Once the transverse momentum of the idler photon is detected at $\vec{q}$, the signal transverse momentum is uniquely detected at $\alpha\vec{q}$, so the above two-photon state is a maximally entangled two-photon state with correlated momentum, namely, a CEPR state. The spectrum function of this state is only determined by $e^{-(1+\alpha)^2 w_0^2 q^2/4}$, which means that the property of the pump's angular spectrum can be transferred to the produced photon pairs. On this point, the case is somewhat similar to that in Ref. [14], in which the longitudinal components of wave vectors are not conserved for the case of a thin crystal and big beam waist of the pump and only the transverse components of wave vectors are conserved, then the correlation in transverse momentum between the signal and the idler photons is still anticorrelated. However, here both the longitudinal and the transverse components of momenta are conserved, which is the key condition for obtaining a perfectly correlated-momentum two-photon state in Eq. (13). Figure 1(a) shows a comparison of phase-matching conditions between the CEPR state and the EPR state.

Furthermore, when the beam waist of the pump w_0 is so small that the pump function E_p can be considered a constant, Eq. (13) becomes $|\Psi\rangle \sim \int d\vec{q}|\vec{q}, \vec{q}\rangle$ ($\alpha = 1$), whose momentum (position) correlation is just reverse to that of the EPR state, so it is called an ideal CEPR state. The physics implicated by this CEPR state is quite different from that of the original EPR state. For the original EPR state, two down-converted photons are born anywhere within the nonlinear crystal from the pump photon simultaneously, and SPDC is considered to be a coherent process. When exiting from the back face of the crystal, the photon pair has the same transverse position but propagating aside the pump with opposite transverse momentum [see Fig. 1(b), right]. The anticorrelated momentum of the original EPR entangled corresponds to a positive correlation of the position at the back face. Once one detects a photon at a certain position of the back face of the crystal, the other should be located at the same position. So the maximally entangled EPR state obeys $\Delta(\vec{q}_s + \vec{q}_i) = 0$ and $\Delta(\vec{\rho}_s - \vec{\rho}_i) = 0$ simultaneously.

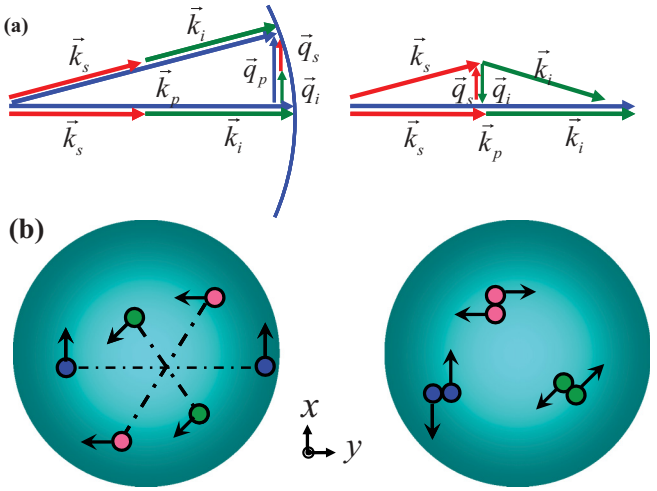

FIG. 1. (Color online) (a) Phase-matching conditions for the CEPR (left) and EPR (right) states. (b) Illustrations of the momentum and position correlations at the output surface of the crystal for the CEPR (left) and EPR (right) states. Actually, for a pair of CEPR photons, their emitting angles are always the same, but they can have all possible values once we detect a pair of photons from two fixed symmetric positions. Here, we only draw a possible angle, for simplicity.

For the CEPR state, the signal and idler are anticorrelated in the transverse position when they exit from the crystal. Through the whole coherent SPDC process, each photon pair can be considered as propagating along the parallel direction but exiting with a centrosymmetric distribution in position [see Fig. 1(b), left]. For the maximally entangled CEPR state, it obeys $\Delta(\vec{q}_s - \vec{q}_i) = 0$ and $\Delta(\vec{\rho}_s + \vec{\rho}_i) = 0$ simultaneously. The difference in the physical picture between the CEPR state and the EPR state is clear now. Because $\vec{q}_s \mp \vec{q}_i$ and $\vec{\rho}_s \pm \vec{\rho}_i$ are not conjugate variables, they can simultaneously have exact values, which does not violate the Heisenberg uncertainty principle, and their product has been proved as a criterion of entanglement [2,3,25]. Actually, for the practical engineering of the CEPR state, since the crystal length cannot be infinitely long and the beam width cannot be infinitely small, it is necessary to assure that the phase-matching bandwidth is much narrower than that of the pump so that

$$\Delta(\vec{q}_s - \vec{q}_i)\Delta(\vec{\rho}_s + \vec{\rho}_i) < 1 \tag{14}$$

is achieved. To verify the CEPR state, it is convenient to take Eq. (14) as the criterion in experiments.

III. THE POSITION CORRELATION OF THE CEPR STATE AT THE OUTPUT CRYSTAL FACE

In this section, we study the position correlation of the CEPR state analytically and numerically. We find a good correspondence between the momentum and the position correlations, i.e., the positive correlation (anticorrelation) of the momentum corresponds to the anticorrelation (positive correlation) of the position on the output surface of a nonlinear crystal. The coincident counting rate R_{cc} at the output face is calculated to be

$$R_{cc} = \lim_{T\to\infty} \frac{1}{T} \int_0^T dt_1 \int_0^T dt_2 |\langle 0|\hat{E}_1^{(+)}(\tau_1)\hat{E}_2^{(+)}(\tau_2)|\psi\rangle|^2, \tag{15}$$

where $\hat{E}_{1,2}^{(+)}$ refers to the positive-frequency component of the free-space electromagnetic field triggered at detector $D_{1,2}$. $\tau_{1,2} = t_{1,2} - \frac{z_{1,2}}{c}$, where $z_{1,2}$ denotes the distance from the output surface of the crystal to the plane of $D_{1,2}$ and $t_{1,2}$ represents the trigger time.

Suppose two detectors are set at the output plane of SPDC, i.e., $z_{1,2} = 0$, $\hat{E}^{(+)}(\tau_{1,2}) = \sum_{\vec{q}_{1,2}} e_\omega \hat{a}(\vec{q}_{1,2},\omega_{1,2}) e^{i\vec{q}_{1,2}\cdot\vec{\rho}_{1,2}} e^{i\omega_{1,2}t_{1,2}}$. For simplicity, we only consider the case where $\alpha = 1$. Define $\vec{q}_\pm = \vec{q}_s \pm \vec{q}_i$ and $\vec{\rho}_\pm = (\vec{\rho}_s \pm \vec{\rho}_i)/2$. Using Eqs. (11) and (15), the coincident counting rate of photon pairs is calculated as

$$R_{cc} \propto \left| \int d\vec{q}_+ E_p(\vec{q}_+) e^{i\vec{q}_+\cdot\vec{\rho}_+} \right|^2 \left| \int d\vec{q}_- H(\vec{q}_-, L) e^{i\vec{q}_-\cdot\vec{\rho}_-} \right|^2. \tag{16}$$

It is clear that the two-photon probability is determined by the Fourier transforms of the pump and the phase-matching functions. The Fourier transform of the pump is $\int d\vec{q}_+ E_p(\vec{q}_+) e^{i\vec{q}_+\cdot\vec{\rho}_+} = \frac{4\pi}{w_0^2} e^{-\rho_+^2/w_0^2}$, and the Fourier transform of the phase-matching function is $\int d\vec{q}_- H(\vec{q}_-, L) e^{i\vec{q}_-\cdot\vec{\rho}_-} = 2\pi k_p/L[\pi - 2Si(k_p\rho_-^2/L)]$, where $\mathrm{Si}(x) \equiv \int_0^x \sin(t)/t dt$. So the coincident counting rate of photon pairs under the noncritical phase-matching condition is

$$R_{cc} \propto e^{-|\vec{\rho}_s+\vec{\rho}_i|^2/2w_0^2} \left(\pi - 2\int_0^{\frac{k_p|\vec{\rho}_s-\vec{\rho}_i|^2}{4L}} \sin t/t dt \right)^2. \tag{17}$$

Figure 2 is a numerical evaluation of the position and momentum correlations under a tightly focused pump with $\xi = 35.81$, respectively. The crystal length $L = 5$ cm and the beam waist $w_0 = 10\ \mu$m. We take the SPDC process of 792 nm ($n_o = 1.759$) $\longrightarrow$ 1584 nm ($n_o = 1.736$) + 1584 nm ($n_e = 1.815$) ($\alpha = 1.05$) at $T = 20^\circ$C in a KTP crystal as the example. n_o or n_e is the refraction index of the pump or entangled photons with o polarization or e polarization. In this case we found that the momenta of a photon pair are positively correlated [see Fig. 2(a)] and the corresponding position correlation shows an anticorrelation [see Fig. 2(b)]. In Fig. 2(a) we also depict the two-photon momentum amplitude A for $q_{sx} = q_{ix}$ [solid (red) line] and $q_{sx} = -q_{ix}$ [dotted (green) line], which reveals the pump mode function E and phase-matching function H in Eq. (11), respectively. As shown in Fig. 2(a), the anticorrelated momentum results from the fact that the bandwidth of the pump

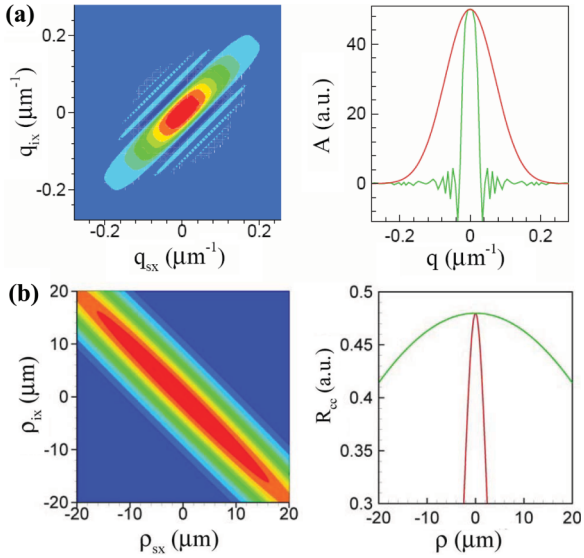

FIG. 2. (Color online) Numerical evaluation of the momentum (a) and position (b) correlations under the condition of $\xi = 35.81$ (crystal length $L = 5$ cm and beam waist $w_0 = 10\ \mu$m). Both the two-photon amplitude $A(q_{sx},q_{ix})$ and the coincidence counting rate R_{cc} are drawn along the x axis, for an obvious comparison of the bandwidth between the pump function and the phase-matching function. We also plot the momentum correlation by setting $q_{sx} = q_{ix}$ [solid (red) line] and $q_{sx} = -q_{ix}$ [dotted (green) line] as shown at the right in (a), where A represents the logogram of the two-photon momentum amplitude $A(q_sx,q_si)$ of Eq. (11). The position correlation is similarly plotted by setting $\rho_{sx} = \rho_{ix}$ [solid (red) line] and $\rho_{sx} = -\rho_{ix}$ [dotted (green) line] as shown at the right in (b).

is much narrower than that of the phase-matching function. Also, when depicting the two-photon counting rate R_{cc} by choosing $\rho_{sx} = \rho_{ix}$ [solid(red) line] and $\rho_{sx} = -\rho_{ix}$ [dotted (green) line], which corresponds to the Fourier transforms of the pump function and phase-matching function as shown in Eq. (17), respectively, we found that the bandwidth of the Fourier transform of the pump function is narrower than that of the Fourier transform of the phase-matching function, so the position correlation is anticorrelated. Here, it is valuable to note that the parameters L and w_0 in the above numerical evaluation still satisfy the noncritical phase-matching condition in Sec. II. For experimental engineering of the CEPR state, some nonlinear crystals with small birefringence are preferred.

IV. THE ENTROPY OF ENTANGLEMENT

In order to quantify the degree of entanglement of the CEPR state, we use the Schmidt decomposition method [28,29]. According to Eq. (11), the two-photon amplitude is $A(\vec{q}_s,\vec{q}_i) = E(\vec{q}_s + \vec{q}_i)H(\vec{q}_s - \vec{q}_i, L)$ ($\alpha = 1$). The Schmidt decomposition of $A(\vec{q}_s,\vec{q}_i)$ corresponds to the signal-sum expansion, i.e., $A(\vec{q}_s,\vec{q}_i) = \sum_{n=0}^{n=\infty} \sqrt{\lambda_n}\mu_n(\vec{q}_s)\nu_n(\vec{q}_i)$, where $\mu_n(\vec{q}_s)$ and $\nu_n(\vec{q}_i)$ are Schmidt modes defined by eigenvectors of the reduced density matrices for the signal and idler photons, respectively, and λ_n are the corresponding eigenvalues. Then the entanglement entropy $S = -\sum_n \lambda_n \log_2 \lambda_n$. For simplicity, we only consider the transverse momentum along the

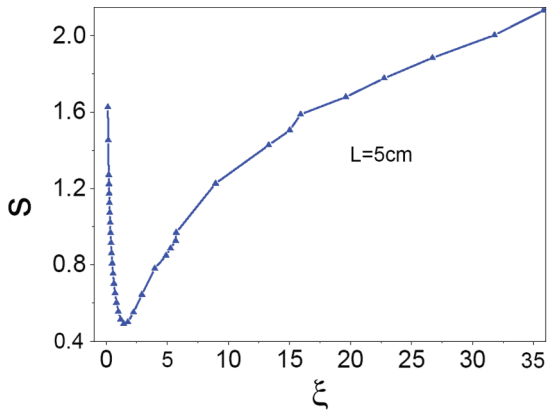

FIG. 3. (Color online) The entanglement entropy S changes with the focal parameter $\xi = L/(w_0^2 k_p)$ for $L = 5$ cm.

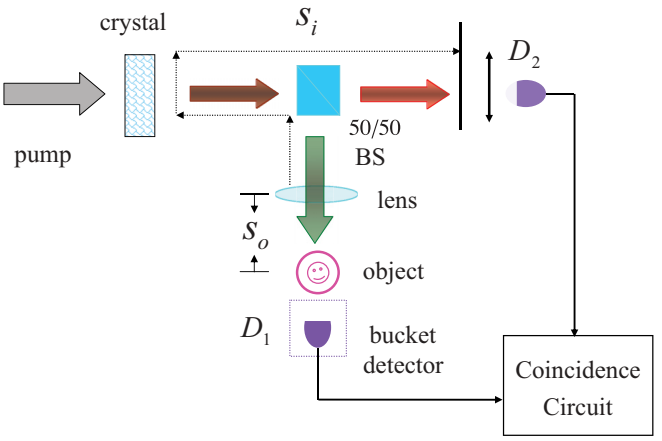

FIG. 4. (Color online) Sketch of the setup for quantum imaging. The CEPR photon pair is beam-split into two paths. A lens is placed in the reflected path and the object followed. Bucket detector D_1 captures all photons passing through the object, and point detector D_2 scans in the transmitted path. The distance between the object and the lens is termed S_o. While the distance between the lens and the crystal plus the distance between the crystal and the second detector is called S_i.

x axis; the calculation of the entanglement entropy is about a scalar quantity and becomes simple.

By the numerical tool for calculating the entropy of entanglement in systems with continuous degrees of freedom [29,30], entropies of entanglement S are calculated and plotted in Fig. 3 (for a summary of mathematical details, see Ref. [29]). We found that the entropies of entanglement S are uniquely determined by the focal parameter ξ despite the actual dimensions of L and w_0, which is consistent with the results in Refs. [18,30]. The demarcation point for the EPR state and CEPR state is $\xi = 1.32$, which corresponds to the minimally entangled state [18]. For $\xi < 1.32$, the two-photon state tends to be an EPR state. An ideal EPR state is achieved when $\xi \ll 1.32$. For CEPR-state generation, we may choose $\xi > 1.32$. Especially when $\xi \gg 1.32$, an ideal CEPR state can be prepared.

It is worth emphasizing that it is difficult to engineer a CEPR state with the same high degree of entanglement as an EPR state. For EPR-state generation we may choose a pump beam waist $w_0 = 1$ mm and a crystal length $L = 2$ mm; in this case $\xi = 1.5 \times 10^{-4}$, and the entanglement entropy is as high as 4.64. For the perfect CEPR-state generation, a long crystal is preferred, while the beam waist of the pump has been minimized to a certain value. In fact, the crystal cannot be infinitely long, or else the third term in the Taylor expansion of $k_{pz} = \sqrt{k_p^2 - q_p^2}$ cannot be neglected, so we have $q_p^4 L/8k_p^3 \ll 1$. Take the maximum value of $q_{\max} = 2/w_0$; this gives that the crystal length $L \ll k_p^3 w_0^4$ or the focal parameter $\xi \ll 2\pi^2(w_0/n_p\lambda)^2$ (n_p is the refractive index of the pump in the crystal). All the parameters we used satisfy this condition. For a reasonable experimental parameter, it is clear that when the crystal length is chosen at several centimeters, one can get a relatively high degree of spatial entanglement. As shown in Fig. 3, for example, if we choose the crystal length $L = 5$ cm, the entropy S can be as high as 2.13 when the beam waist of the pump is chosen as $w_0 = 10$ μm.

V. QUANTUM GHOST IMAGING BASED ON THE IDEAL CEPR STATE

Besides the fundamental interest in the CEPR state, its potential applications are diverse due to its new characteristics in momentum and position correlations. Quantum imaging is calculated when using the CEPR state. The schematic for the setup of quantum ghost imaging is shown in Fig. 4. When doing coincidence counting between two detectors, the image will be retrieved. The electric field at the mth detector can be described by Green's function $G_m(m = 1,2)$, which describes the propagation of the beam through the optical system [27]. The two-photon amplitude is

$$A(\vec{\rho}_1,\vec{\rho}_2) = \int d\vec{q}_1 \int d\vec{q}_2 e^{-i(\omega_1 t_1+\omega_2 t_2)} G_1(\vec{q}_1,\omega_1;\vec{\rho}_1,z_1) \times G_2(\vec{q}_2,\omega_2;\vec{\rho}_2,z_2)\langle 0|\hat{a}(\vec{q}_1,\omega_1)\hat{a}(\vec{q}_2,\omega_2)|\Psi\rangle, \quad (18)$$

where $G_1(\vec{q}_1,\omega_1;\vec{\rho}_1,z_1) = \int d\vec{\rho}_{s1} \int d\vec{\rho}_f h_\omega(\vec{\rho}_1 - \vec{\rho}_f, s_o) S(\vec{\rho}_f)$ $h_\omega(\vec{\rho}_f - \vec{\rho}_{s1}, z_1 - s_o) e^{i\vec{q}_1\cdot\vec{\rho}_{s1}}$ and $G_2(\vec{q}_2,\omega_2;\vec{\rho}_2,z_2) = \int d\vec{\rho}_{s2} h_\omega$ $(\vec{\rho}_2 - \vec{\rho}_{s2}, z_2) e^{i\vec{q}_2\cdot\vec{\rho}_{s2}}$, in which the optical transfer function h_ω is defined as $h_\omega(\vec{\rho},z) = \frac{-i\omega}{2\pi c}\frac{e^{i\frac{\omega z}{c}}}{z} e^{i\frac{\omega\rho^2}{2cz}}$ in the paraxial approximation, and $S(\vec{\rho}_f) = e^{-i\frac{\omega\rho_f^2}{2cf}} t(\vec{\rho}_f)$. s_o represents the distance between the object and the lens, and $\vec{\rho}_{s1(2)}$ denotes position 1 or 2 of the crystal back face. $\vec{\rho}_{1,2}$ ($\vec{q}_{1,2}$) represents the transverse position (momentum) of the first or second detector, respectively. $z_{1,2}$ represents the distance between the first or second detector and the corresponding position at the back face of the crystal.

Assume that the lens in the object path is infinite and its transmitting function $t(\vec{\rho}) = 1$, the two-photon amplitude in Eq. (18) becomes

$$A_{12} \propto \delta\left(\vec{\rho}_1 - \frac{S_o}{S_i}\vec{\rho}_2\right), \quad (19)$$

where $\frac{1}{S_o} + \frac{1}{S_i} = \frac{1}{f}$ [$S_{o(i)}$ is marked in Fig. 4] is satisfied, and $\frac{S_i}{S_o}$ represents the magnification of the object. It is noticeable that quantum imaging using CEPR two-photon pairs is an

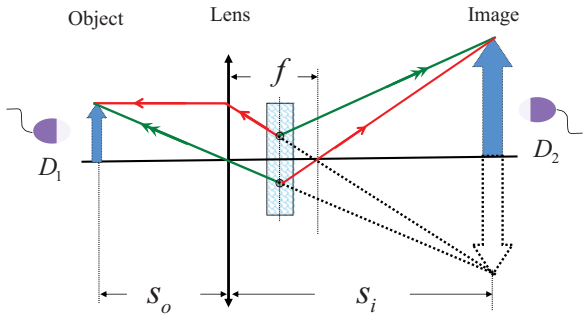

FIG. 5. (Color online) The conceptual "unfolded" version of quantum imaging using CEPR photon pairs (erect image) and EPR photon pairs (headstand image). S_o and S_i represent distances of the object and image, respectively.

upright one, which is different from the headstand imaging using original EPR photon pairs. When the lens is placed satisfying the imaging condition given by the thin lens formula $\frac{1}{S_o}+\frac{1}{S_i}=\frac{1}{f}$, the image is well produced in the joint detection (see Fig. 4). Considering quantum imaging using original EPR photon pairs, the advanced wave picture states that the crystal plays the role of a reflecting mirror in the imaging process. This is guaranteed by the anticorrelated momentum and correlated position of the entangled photon pair as shown by the unfolded layout in Fig. 5 (dashed line) [5]. The unfolded ghost imaging by CEPR photon pairs is also shown in Fig. 5 (solid line), the anticorrelated-position and correlated-momentum result in an upright image, which also embodies the calculating process of Eq. (19). Here, it is notable that the upright image can serve as a criterion for the CEPR state existing in experiments. Just as calculated in Ref. [25], when the object is a symmetric double slit, the ghost image cannot distinguish the CEPR state and the EPR state. But for a nonsymmetric object or an object deviating from the pump's center, the ghost image using two types of states is different. However, as discussed in Sec. IV, the generation of a CEPR state with a high degree of entanglement is not easy; this may reduce the resolution in quantum imaging.

VI. CONCLUSION

In summary, in this paper we propose to engineer the counterpart of the EPR state directly from nonlinear crystals. The pump focal parameter uniquely determines the wave function, momentum, and position correlations and the entanglement entropy of such CEPR photon pairs. This type of CEPR state may attract fundamental interest and stimulate possible applications in quantum technology and quantum information science. For quantum imaging, we calculate and find an erect ghost imaging based on this CEPR state. Other new applications are still under investigation.

ACKNOWLEDGMENTS

This work was supported by the State Key Program for Basic Research of China (Grants No. 2012CB921802 and No. 2011CBA00205), the National Natural Science Foundations of China (Grants No. 11174121, No. 91121001, No. 11004096, and No. 11021403), and the Project Funded by the Priority Academic Program Development of Jiangsu Higher Education Institutions (PAPD).

[1] A. Einstein, B. Podolsky, and N. Rosen, Phys. Rev. **47**, 777 (1935).
[2] M. D'Angelo, Y. H. Kim, S. P. Kulik, and Y. H. Shih, Phys. Rev. Lett. **92**, 233601 (2004).
[3] J. C. Howell, R. S. Bennink, S. J. Bentley, and R. W. Boyd, Phys. Rev. Lett. **92**, 210403 (2004).
[4] M. D. Reid, P. D. Drummond *et al.*, Rev. Mod. Phys. **81**, 1727 (2009).
[5] T. B. Pittman, Y. H. Shih, D. V. Strekalov, and A. V. Sergienko, Phys. Rev. A **52**, R3429 (1995).
[6] R. S. Bennink, S. J. Bentley, R. W. Boyd, and J. C. Howell, Phys. Rev. Lett. **92**, 033601 (2004).
[7] A. Gatti, E. Brambilla, and L. A. Lugiato, Phys. Rev. Lett. **90**, 133603 (2003).
[8] A. N. Boto, P. Kok, D. S. Abrams, S. L. Braunstein, C. P. Williams, and J. P. Dowling, Phys. Rev. Lett. **85**, 2733 (2000).
[9] M. D'Angelo, M. V. Chekhova, and Y. H. Shih, Phys. Rev. Lett. **87**, 013602 (2001).
[10] Y. Kawabe, H. Fujiwara, R. Okamoto *et al.*, Opt. Express **15**, 14244 (2007).
[11] T. Nagata, R. Okamoto, J. L. O'Brien, K. Sasaki, and S. Takeuchi, Science **316**, 726 (2007).
[12] V. Giovannetti, S. Lloyd, and L. Maccone, Nature Photon. **5**, 222 (2011).
[13] W. B. Gao, P. Xu, X. C. Yao, O. Gühne, A. Cabello, C. Y. Lu, C. Z. Peng, Z. B. Chen, and J. W. Pan, Phys. Rev. Lett. **104**, 020501 (2010).
[14] C. H. Monken, P. H. Souto Ribeiro, and S. Pádua, Phys. Rev. A **57**, 3123 (1998).
[15] P. S. K. Lee, M. P. van Exter, and J. P. Woerdman, Phys. Rev. A **72**, 033803 (2005).
[16] S. P. Walborn and C. H. Monken, Phys. Rev. A **76**, 062305 (2007).
[17] S. P. Walborn, C. H. Monken, S. Pádua, and P. H.Souto Ribeiro, Phys. Rep. **495**, 87 (2010).
[18] W. P. Grice, R. S. Bennink, D. S. Goodman, and A. T. Ryan, Phys. Rev. A **83**, 023810 (2011).
[19] H. Di Lorenzo Pires, F. M. G. J. Coppens, and M. P. van Exter, Phys. Rev. A **83**, 033837 (2011).
[20] W. A. T. Nogueira, S. P. Walborn, S. Pádua, and C. H. Monken, Phys. Rev. Lett. **86**, 4009 (2001).
[21] A. Vaziri, G. Weihs, and A. Zeilinger, J. Opt. B **4**, S47 (2002).
[22] L. Neves, G. Lima, J. G. Aguirre Gómez, C. H. Monken, C. Saavedra, and S. Pádua, Phys. Rev. Lett. **94**, 100501 (2005).
[23] A. Valencia, A. Ceré, X. J. Shi, G. Molina-Terriza, and J. P. Torres, Phys. Rev. Lett. **99**, 243601 (2007).
[24] G. Lima *et al.*, Opt. Express **17**, 10688 (2009).
[25] W. T. Liu, P. X. Chen, C. Z. Li, and J. M. Yuan, Phys. Rev. A **79**, 061802 (2009).

[26] R. W. Boyd, *Nonlinear Optics* (Academic Press, Boston, 1992).
[27] M. H. Rubin, Phys. Rev. A **54**, 5349 (1996).
[28] C. K. Law, I. A. Walmsley, and J. H. Eberly, Phys. Rev. Lett. **84**, 5304 (2000).
[29] S. Parker, S. Bose, and M. B. Plenio, Phys. Rev. A **61**, 032305 (2000).
[30] C. K. Law and J. H. Eberly, Phys. Rev. Lett. **92**, 127903 (2004).